

Tritium Conductivity and Isotope Effect in Proton-Conducting Perovskites

R. Mukundan,^{a,*} Eric L. Brosha,^{a,*} Stephen A. Birdsell,^b Alison L. Costello,^b
Fernando H. Garzon,^{a,*} and R. Scott Willms^b

Los Alamos National Laboratory, ^aElectronic and Electrochemical Materials and Devices Group, ^bTritium Science and Engineering Group, Los Alamos, New Mexico 87545, USA

The tritium ion conductivities of SrZr_{0.9}Yb_{0.1}O_{2.95} and BaCe_{0.9}Yb_{0.1}O_{2.95} have been measured by ac impedance analysis. The high tritium conductivity of these perovskites could potentially lead to their application as an electrochemical membrane for the recovery of tritium from tritiated gas streams. The conductivities of these perovskites, along with SrCe_{0.95}Yb_{0.05}O_{2.975}, were also measured in hydrogen- and deuterium-containing atmospheres to illustrate the isotope effect. For the strontium zirconate and barium cerate samples, the impedance plot consists of two clearly resolved arcs, a bulk and a grain boundary arc, in the temperature range 50-350°C. However, for the strontium cerate sample, the clear resolution of the bulk conductivity was not possible and only the total conductivity was measurable. Thus, the isotope effect was clearly established only for the strontium zirconate and barium cerate samples. The decrease in bulk conductivity with increasing isotope mass was found to be a result of an increase in the activation energy for conduction accompanied by a decrease in the pre-exponential factor. Since the concentration of the mobile species (H⁺, D⁺, or T⁺) should remain relatively constant at T < 350°C, this increase in activation energy is directly attributable to the increased activation energy for the isotope mobility.

© 1999 The Electrochemical Society. S0013-4651(98)07-113-4. All rights reserved.

Manuscript received July 31, 1998.

High temperature protonic-conducting oxides based on the perovskite structure have been studied extensively since their discovery in 1981.¹ The hydrogen and deuterium isotope conductivities in these oxides have been evaluated^{2,3} recently, and their potential application as hydrogen separation membranes has been discussed.⁴ However, there are no reported studies on the tritium ion-conduction in these perovskites. In this paper, we report the hydrogen (H), deuterium (D), and tritium (T) conductivities of three protonic conducting perovskites, viz. SrZr_{0.9}Yb_{0.1}O_{2.95}, BaCe_{0.9}Yb_{0.1}O_{2.95}, and SrCe_{0.95}Yb_{0.05}O_{2.975}. The conductivity of tritium ions through these perovskites not only gives fundamental information regarding the hydrogen transport in these perovskites, but also allows for the exciting possibility of tritium separation using these oxides as an electrochemical membrane.

The proton-conducting compounds that were investigated in this study were selected for the following reasons. (1) The strontium zirconates are known to have the best chemical stability in CO₂ containing atmospheres (stable in 20 vol % CO₂ at 700°C).⁵ (2) The barium cerates have one of the highest magnitudes of protonic conductivity.⁶ (3) The strontium cerates, having a high protonic transference number, are the most extensively studied proton-conducting perovskites.⁷⁻⁹

Although a H/D isotope effect has been shown in proton-conducting perovskites, the data in the literature is neither extensive nor consistent enough to clearly establish a model for protonic conduction in these perovskites.² The measured difference in activation energies for the H- and D-ion conduction has eliminated the possibility of proton hopping governed by a classical theory and has given support to a semiclassical approach. This approach takes into consideration the difference in zero point energies between the ground state of H and D, given by Eq. 1¹⁰

$$E_D - E_H = \frac{1}{2} h(\nu_D - \nu_H) \quad [1]$$

where E_H and E_D are the activation energies for the H- and D-ion conduction, respectively, and ν_H and ν_D are the OH and OD stretching frequencies. However the pre-exponential factors presented in the literature do not obey the predictions of the semiclassical theory given by Eq. 2

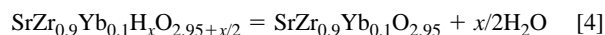
$$A_{H/D/T} = z\lambda^2 e^2 \nu_{H/D/T} c_{\text{eff}} / 6vk \text{ and } A_H/A_D = \sqrt{2} \text{ and } A_H/A_T = \sqrt{3} \quad [2]$$

Where $z = 8$ (number of jump directions), $\lambda =$ jump distance (O-O distance), $c_{\text{eff}} =$ concentration of mobile protons, and $\nu =$ unit cell volume. In this paper, we present the H-, D-, and T-ion conductivities of SrZr_{0.9}Yb_{0.1}O_{2.95} and BaCe_{0.9}Yb_{0.1}O_{2.95}, and attempt to explain the various factors that need to be addressed in order to unambiguously determine the conduction mechanism in these perovskites.

Experimental

Single-phase perovskite samples of SrZr_{0.9}Yb_{0.1}O_{2.95}, BaCe_{0.9}Yb_{0.1}O_{2.95}, and SrCe_{0.95}Yb_{0.05}O_{2.975} were prepared using standard solid-state methods by heating appropriate stoichiometric mixtures of BaCO₃, SrCO₃, CeO₂, ZrO₂, and Yb₂O₃ at 1773 K for 20 h with two intermediate ballmilling steps. The formation of a single-phase orthorhombic perovskite was confirmed by powder X-ray diffraction using a Siemens D 5000 diffractometer. Dense ceramic samples (typically $\geq 95\%$ theoretical) were obtained by isostatically pressing the powders into pellets at 35 MPa for 5 min, and sintering at 1923 K for 10 h. Samples were then cut out of these pellets for thermogravimetric analysis (TGA) and conductivity measurements.

The thermogravimetric analysis was performed using a Perkin Elmer TGA 7 analyzer. The sintered samples were first treated in either 2% H₂/3% H₂O/argon or 2% D₂/3% D₂O/argon gas mixtures at 600°C for 24 h and furnace cooled to room temperature. This treatment leads to the incorporation of protons or deuterons into the sample. The protonated (deuterated) samples were then heat-treated at 1000°C for 16 h in ultrahigh purity argon and the weight loss was monitored. This weight loss was attributed to the loss of H₂O or D₂O from the sample¹¹ according to Eq. 3-5



For the ac impedance measurements, the samples were painted with porous platinum ink on two sides and loaded onto an alumina holder with Pt leads. The measurements were performed using a Solartron 1260 impedance analyzer, in the frequency range from 10 mHz to 13 MHz. For the tritium measurements, the sample along with the holder was sealed in a quartz tube and the setup was kept in a glove box for secondary containment. The tritium level in the glove

* Electrochemical Society Active Member.

^z E-mail: mukundan@lanl.gov

Table I. Proton and deuteron concentrations measured by TGA.

Chemical composition	X, when quenched from 600°C in 2% H ₂ /3% H ₂ O/argon; and percent occupancy of oxygen vacancies	X, when quenched from 600°C in 2% D ₂ /3% D ₂ O/argon and percent occupancy of oxygen vacancies
SrCe _{0.95} Yb _{0.05} (H/D) _x O _{2.975+x/2}	H = 0.01 ± 0.005 (20%)	D = 0.01 ± 0.005 (20%)
SrZr _{0.9} Yb _{0.1} (H/D) _x O _{2.95+x/2}	H = 0.02 ± 0.005 (20%)	D = 0.02 ± 0.005 (20%)
BaCe _{0.9} Yb _{0.1} (H/D) _x O _{2.95+x/2}	H = 0.04 ± 0.005 (40%)	D = 0.04 ± 0.005 (40%)

box was continuously monitored to check for any tritium leaks. The setup was then heated to 600°C under vacuum and the primary containment was leak checked. A 2% T₂/argon gas mixture (0.76 atm, atmospheric pressure at Los Alamos) was introduced into the setup which was then isolated from the tritium supply. The conductivity was monitored every half-hour for a total of 6 h to confirm the tritium incorporation into the sample. The sample was then cooled to room temperature and conductivity measurements were performed every 50°C, from 50 to 350°C. This procedure was followed in order to minimize and contain the amount of tritium used in the experiment. However, for the H₂ and D₂ measurements, the samples were heat-treated in 2% H₂/3% H₂O/argon or 2% D₂/3% D₂O/argon gas mixtures, respectively, at 600°C for 24 h and then furnace cooled to room temperature. Moreover, the H₂ and D₂ conductivity measurements were performed in the flowing gas mixture in the temperature range from 50 to 350°C.

Results and Discussion

The results of the TGA are summarized in Table I, which shows that the concentration of protons and deuterons are identical under the treatment conditions used. The maximum proton occupancy was observed for the barium cerate sample (40%) and the minimum for strontium cerate (20%). This observation is consistent with the fact that the barium cerate sample has the highest magnitude of protonic conductivity whereas the strontium cerate has the lowest conductivity. This is also reflective of the fact that the strontium cerate has only 5% Yb dopant, and hence, only 2.5% oxygen vacancies that can incorporate protons in the wet state. Moreover, the measured concentration of protons agrees well with the values of 20-40% reported for several proton-conducting perovskites under similar conditions.¹¹⁻¹³

The total conductivity of these materials consists of a bulk (lattice conductivity) and a grain-boundary contribution. However, for the strontium cerate sample, there is a significant overlap in the bulk and grain boundary conductivities as shown in Fig. 1. Using the Boukamp-University of Twente EQUIVCRT software, two distinct

arcs could be fitted to this data (Fig. 1). However, when the protonic conductivity of three different samples were analyzed thus, the scatter in the data was large. For example, 0.57 < ΔH_H < 0.63, and 700 < A_H < 3000. Although this scatter in activation energy values makes it difficult to determine an isotope effect, it is consistent with that reported in the literature,¹⁴ where 0.55 eV < ΔH_H < 0.63.

This large scatter in activation energy (±0.06 eV), in both our data and in that available in the literature, is primarily due to two factors. The first factor is the variation of proton concentration with changing temperature and the second is the contribution of the grain boundary conductivity. While the first factor is predominant at elevated temperatures (>600°C) where the concentration of protons in the sample tends to decrease due to water evolution from the sample,¹⁵ the second factor is predominant at the lower temperature regime (<600°C) where the grain boundary conductivity is significant.

In order to study the former effect independent of the latter, it is necessary to determine the bulk conductivity at elevated temperatures. This was accomplished by using a SrZr_{0.9}Yb_{0.1}O_{2.95} sample with a high value of resistance (l/A = 9.36). The impedance spectra of this sample at 600°C is plotted in Fig. 2 along with the impedance spectra of a sample with l/A = 0.212 at 300°C. This large difference (44 times) in the resistance of the two samples allows for the determination of the bulk conductivity over a wide temperature regime. While the latter sample (l/A = 0.212) was used for the determination of the bulk conductivity at low temperatures (<350°C), the former (l/A = 9.36) was used to resolve the bulk conductivity at high temperatures (>300°C). This high temperature bulk conductivity is plotted in Fig. 3, which shows a decrease in the protonic conductivity with increasing temperature at T > 600°C. This is the result of a decrease in the proton concentration in the sample; any activation energy measured from this data is not representative of the proton mobility in the sample, and hence, will not be useful in determining isotopic effects.

The second factor, the contribution of the grain boundary, can be illustrated by observation of the conductivity in the lower temperature regime. Note from the impedance spectra of Fig. 2 that the grain boundary conductivity is predominant only in the low temperature

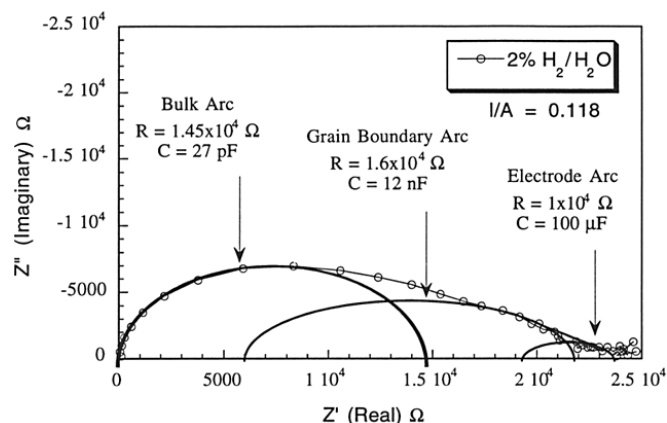


Figure 1. AC impedance plot of SrCe_{0.95}Yb_{0.05}O_{2.975} at 250°C. The circles drawn in the figure are for clarity only and are not actual representation of the circuit elements.

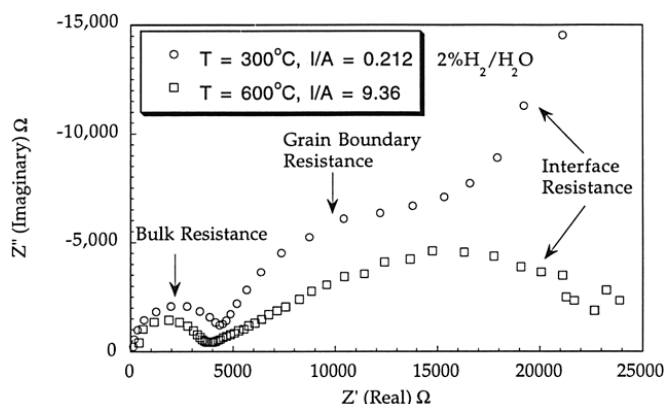


Figure 2. The impedance data obtained from two different samples of SrZr_{0.9}Yb_{0.1}O_{2.95} at two different temperatures. The sample with l/A = 9.36 has a resistance that is 44 times that of the sample with the l/A = 0.212.

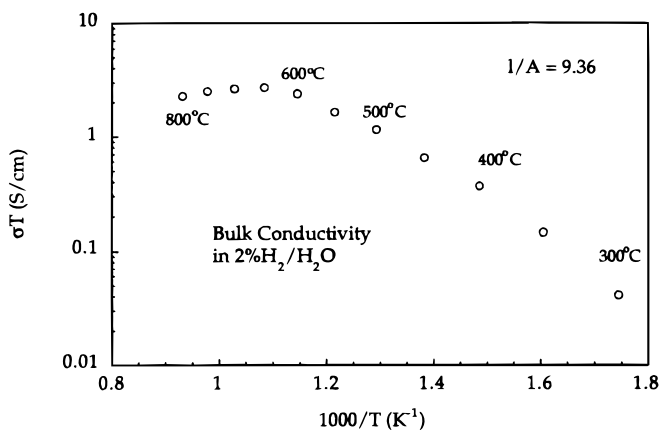


Figure 3. Arrhenius plot of the bulk conductivity of SrZr_{0.9}Yb_{0.1}O_{2.95} in a 2% H₂/3% H₂O/argon atmosphere.

regime (the grain boundary contribution is negligible at 600°C). The bulk and grain boundary conductivities of SrZr_{0.9}Yb_{0.1}O_{2.95} in this temperature regime (100–400°C) are plotted in Fig. 4. It can be seen that the activation energy for the total conductivity (0.84 eV) is significantly different from that of the bulk (0.56 eV).

Apart from these two factors, there could be additional error introduced due to the hole and oxygen-ion conductivity in these perovskites. Typically, the hole and oxygen-ion conductivities have higher activation energies and tend to dominate at elevated temperatures.¹⁶ Hence, it is imperative that the bulk and grain boundary contributions be resolved clearly, and also the measurements be performed at a low enough temperature range so as to keep the proton concentration constant. This was possible for both the SrZr_{0.9}Yb_{0.1}O_{2.95} and BaCe_{0.9}Yb_{0.1}O_{2.95} samples; and these were utilized to illustrate the isotopic effect in these proton conductors.

The impedance spectra of the BaCe_{0.9}Yb_{0.1}O_{2.95} sample at 150°C in H₂-, D₂-, and T₂-containing atmospheres is shown in Fig. 5. The bulk and grain boundary contributions to the conductivity could be clearly resolved from this spectra. For this sample as well as the SrZr_{0.9}Yb_{0.1}O_{2.95} sample, the measured ΔH for two different batches of samples were within ± 0.01 eV and were used to illustrate the isotopic effect. However, the corresponding error in the pre-exponential factor is still as high as 25%. The bulk (lattice) isotope conductivities of BaCe_{0.9}Yb_{0.1}O_{2.95} and SrZr_{0.9}Yb_{0.1}O_{2.95} are plotted in Fig. 6a and b along with the fitted values of activation energies and pre-exponential factors. The tritium conductivity data which have been reported for the first time in the literature confirm the increasing activation energy with increasing isotope mass for the

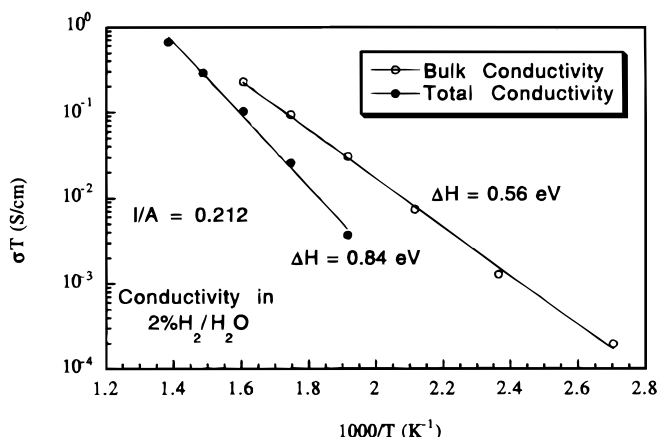


Figure 4. Arrhenius plot of the bulk and total conductivity of SrZr_{0.9}Yb_{0.1}O_{2.95} in a 2% H₂/3% H₂O/argon atmosphere.

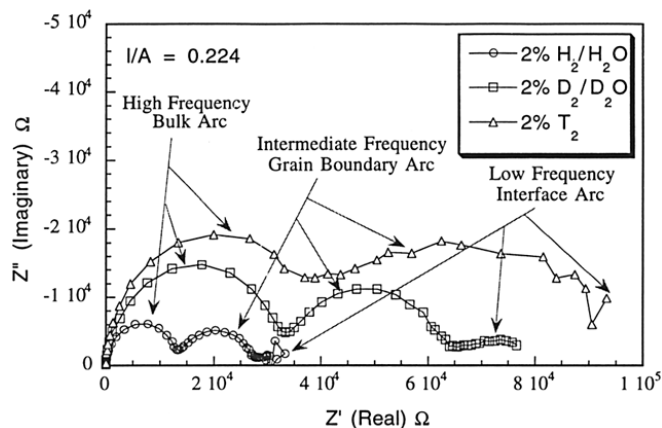


Figure 5. AC impedance plot of BaCe_{0.9}Yb_{0.1}O_{2.95} at 150°C.

SrZr_{0.9}Yb_{0.1}O_{2.95} sample ($\Delta H_H = 0.56$ eV, $\Delta H_D = 0.58$ eV, $\Delta H_T = 0.61$ eV). However, for the BaCe_{0.9}Yb_{0.1}O_{2.95} sample, the change in ΔH between the D₂ and T₂ measurements is within the experimental error ($\Delta H_H = 0.55$ eV, $\Delta H_D = 0.57$ eV, $\Delta H_T = 0.56$ eV). This could be due to the lower concentration of T₂ in the sample, and hence, some interference due to p-type conductivity which is known to be high in barium cerates.¹⁶ This problem can be mitigated by the incorporation of tritium using T₂/T₂O/argon mixtures instead of T₂/argon mixtures. However, this experiment was not attempted due to the high risk (human radiological hazard) involved in using tritiated water.

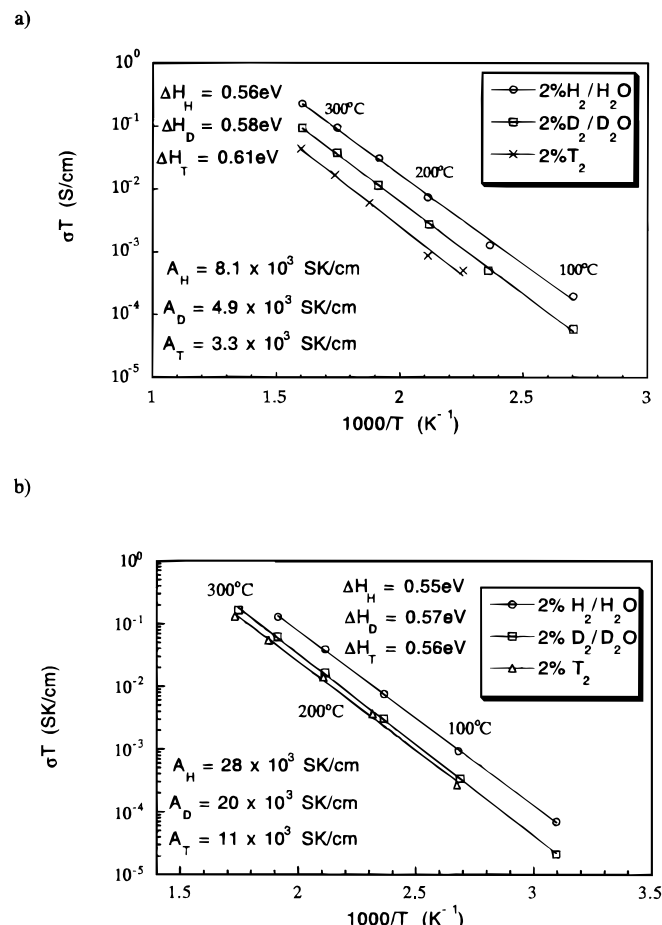


Figure 6. Arrhenius plot of the conductivity of (a) SrZr_{0.9}Yb_{0.1}O_{2.95} and (b) BaCe_{0.9}Yb_{0.1}O_{2.95} in H₂-, D₂-, and T₂-containing atmospheres.

From Fig. 6a and b it can be seen that the pre-exponential factor decreases with increasing isotope mass. Moreover, the ratios of $A_{\text{H}}/A_{\text{D}}$ (1.65 and 1.4) and $A_{\text{H}}/A_{\text{T}}$ (2.45 and 2.55) are consistent with the semiclassical theory and within experimental error, close to $\sqrt{2}$ and $\sqrt{3}$, respectively. The larger than $\sqrt{3}$ ratio observed for $A_{\text{H}}/A_{\text{T}}$ could be a result of a lower concentration of tritium incorporated into the sample. However, given the high uncertainty (50%) in the ratios of the pre-exponential factor, it would be more instructive to fit the observed values of $A_{\text{H/D/T}}$ to Eq. 2 in order to confirm the mechanism of proton migration in these perovskites. This has been attempted in the literature² using a value of 10^{14} s^{-1} for ν_{H} as determined from single crystal studies of KTaO_3 .¹⁷ However, a precise evaluation of the pre-exponential factors requires the direct determination of ν_{H} , ν_{D} , and ν_{T} values in these perovskites. Experiments to accomplish this using inelastic neutron scattering are planned for the future.

Conclusions

The measured tritium-ion conductivities of $\text{BaCe}_{0.9}\text{Yb}_{0.1}\text{O}_{2.95}$ and $\text{SrZr}_{0.9}\text{Yb}_{0.1}\text{O}_{2.95}$ are consistent with a semiclassical model for the proton migration. The reasonably high values of tritium conductivity (bulk + grain boundary) measured for the $\text{BaCe}_{0.9}\text{Yb}_{0.1}\text{O}_{2.95}$ ($\sigma_{\text{T}} = 1 \text{ mS/cm}$ at 600°C) and $\text{SrZr}_{0.9}\text{Yb}_{0.1}\text{O}_{2.95}$ ($\sigma_{\text{T}} = 0.7 \text{ mS/cm}$ at 600°C) samples could lead to their application as tritium separation membranes. These electrochemical reactors could have potential application in tritium recycling, environmental clean up and waste mitigation of tritiated water and hydrocarbons.

Acknowledgment

Los Alamos National Laboratory is operated by the University of California for the U.S. Department of Energy under contract W-7405-ENG-36.

Los Alamos National Laboratory assisted in meeting the publication costs of this article.

References

1. H. Iwahara, T. Esaka, H. Uchida, and N. Maeda, *Solid State Ionics*, **3/4**, 359 (1981).
2. A. S. Nowick and A. V. Vaysleyb, *Solid State Ionics*, **97**, 17 (1997).
3. T. Hibino, K. Mizutani, and H. Iwahara, *J. Electrochem. Soc.*, **140**, 2588 (1993).
4. H. Iwahara, *Solid State Ionics*, **77**, 289 (1995).
5. T. Yajima, H. Iwahara, K. Koide, and K. Yamamoto, *Sens. Actuators, B*, **5**, 145 (1991).
6. D. A. Stevenson, N. Jiang, R. M. Buchanan, and F. E. G. Henn, *Solid State Ionics*, **62**, 279 (1993).
7. T. Scherban and A. S. Nowick, *Solid State Ionics*, **35**, 189 (1989).
8. T. Yamajima and H. Iwahara, *Solid State Ionics*, **53-56**, 983 (1992).
9. T. Schober, J. Friedrich, and J. B. Condon, *Solid State Ionics*, **77**, 175 (1995).
10. W.-K. Lee, A. S. Nowick, and L. A. Boatner, *Solid State Ionics*, **18/19**, 989 (1986).
11. H. Uchida, H. Yoshikawa, and H. Iwahara, *Solid State Ionics*, **35**, 229 (1989).
12. H. Hibino, K. Mizutani, T. Yajima, and H. Iwahara, *Solid State Ionics*, **57**, 303 (1992).
13. J. F. Liu and A. S. Nowick, *Solid State Ionics*, **50**, 131 (1992).
14. M. Zheng and B. Zhu, *Solid State Ionics*, **80**, 59 (1995).
15. T. Yajima and H. Iwahara, *Solid State Ionics*, **53-56**, 983 (1992).
16. N. Bonanos, *Solid State Ionics*, **53-56**, 967 (1992).
17. S. Q. Fu, W.-K. Lee, A. S. Nowick, L. A. Boatner, and M. M. Abraham, *J. Solid State Chem.*, **83**, 221 (1989).